Special Supplement: Pulses

Image-based modeling in the selection of cowpea genotypes for aluminum tolerance[1]

Uasley Caldas de Oliveira[2], Janderson do Carmo Lima[3],
Robson de Jesus Santos[2], Vitor Oliveira dos Santos[2], Marilza Neves do Nascimento[2]

ABSTRACT

In acidic soils, one of the main factors limiting crop yield is the presence of aluminum. However, some species may exhibit tolerance and mitigate the toxic effects of this element. This study aimed to evaluate and compare machine learning algorithms for the predictive analysis of aluminum ion accumulation sites, using the Evans blue dye to assess its interaction with root morphology, in cowpea genotypes. A completely randomized design, with five aluminum concentrations (0, 50, 100, 150 and 200 µM of $AlCl_3 \cdot 6H_2O$) and fourteen cowpea genotypes, was used. Significant variations in aluminum tolerance were observed among the genotypes, with MNC06-908-39 and MNC06-895-1 being classified as the most sensitive, whereas MNC06-907-29 and MNC06-901-14 exhibited a higher tolerance. CB-27 was identified as the most tolerant overall, whereas MNC06-909-54, MNC06-909-55, MNC06-907-35, MNC06-908-39 and MNC06-909-76 were considered the highest sensitive ones. The quantitative dye analysis corroborated the qualitative findings, confirming the higher aluminum tolerance of the MNC06-907-29 and MNC06-901-14 genotypes, whereas MNC06-908-39 and MNC06-895-1 were the most sensitive ones. A predictive analyses, using the Random Forest, Decision Tree, k-Nearest Neighbors and Neural Network algorithms, demonstrated a clear genetic variability among the genotypes in response to aluminum stress, with the Neural Network showing the highest predictive accuracy.

KEYWORDS: *Vigna unguiculata* L., abiotic stress, machine learning.

RESUMO

Modelagem baseada em imagens na seleção de genótipos de feijão-caupi para tolerância a alumínio

Em solos ácidos, um dos principais agentes que afetam a produtividade das culturas é a presença de alumínio. Entretanto, algumas espécies podem apresentar tolerância e mitigar os efeitos tóxicos desse elemento. Objetivou-se avaliar e comparar algoritmos de aprendizado de máquina na análise preditiva de sítios de acúmulo de íon alumínio, empregando-se o corante Evans blue para avaliar sua interação com a morfologia radicular, em genótipos de feijão-caupi. Utilizou-se delineamento casualizado, com cinco doses de alumínio (0, 50, 100, 150 e 200 µM de $AlCl_3 \cdot 6H_2O$) e quatorze genótipos de feijão-caupi. Diferenças significativas na tolerância ao alumínio foram observadas entre os genótipos, com destaque para MNC06-908-39 e MNC06-895-1, classificados como os mais sensíveis, enquanto MNC06-907-29 e MNC06-901-14 apresentaram maior tolerância. CB-27 foi identificado como o mais tolerante, enquanto MNC06-909-54, MNC06-909-55, MNC06-907-35, MNC06-908-39 e MNC06-909-76 foram categorizados como os mais sensíveis. A quantificação do corante corroborou os resultados qualitativos, confirmando que MNC06-907-29 e MNC06-901-14 apresentaram maior tolerância ao alumínio, enquanto MNC06-908-39 e MNC06-895-1 exibiram maior sensibilidade. Uma análise preditiva, realizada por meio dos algoritmos Random Forest, Decision Tree, k-Nearest Neighbors e Neural Network, revelou evidente variabilidade genética entre os genótipos, quanto à tolerância ao alumínio, sendo que o Neural Network apresentou o melhor desempenho preditivo.

PALAVRAS-CHAVES: *Vigna unguiculata* L., estresse abiótico, aprendizado de máquina.

INTRODUCTION

Cowpea [*Vigna unguiculata* (L.) Walp.] is a vital dietary component for populations worldwide and is cultivated by both smallholder and large-scale producers (FAO 2017). In Brazil, however, the production in the 2021/2022 season reached only 36.6 thousand tons, with yields ranging from 0.4 to 1.5 t ha^{-1} - values well below the crop's potential (FAO 2017). These figures are especially low when

[1] Received: May 17, 2025. Accepted: July 17, 2025. Published: Aug. 27, 2025. DOI: 10.1590/1983-40632025v5582693.
[2] Universidade Estadual de Feira de Santana, Departamento de Biologia, Feira de Santana, BA, Brazil.
E-mail/ORCID: uasley@gmail.com/0000-0001-6551-7746; robssantos17@hotmail.com/0000-0003-4917-6683; vitor.agro.uefs@gmail.com/0009-0001-3053-0876; mnnascimento@uefs.br/0000-0003-3344-9106.
[3] Universidade Estadual de Goiás, Instituto Acadêmico de Ciências Agrárias e Sustentabilidade, Posse, GO, Brazil.
E-mail/ORCID: janderson.lima@ueg.br/0000-0002-7564-5044.
Editor: Luis Carlos Cunha Junior

compared to technologically advanced agricultural countries such as the United States, where yields exceed 1.5 t ha^{-1} (FAO 2017, Conab 2018).

One of the main factors limiting cowpea yield in Brazil is the high level of aluminum saturation in the soil, a global constraint to agricultural production (Kochian et al. 2015, Eekhout et al. 2017), particularly in regions with intensely weathered soils, as found in Brazil. Aluminum toxicity predominantly affects the root system, where the metal binds to the epidermal and cortical root cells due to its high reactivity. This interaction compromises the plasma membrane, cell wall, nucleus and cytoskeleton, ultimately causing cell damage (Hassanpour et al. 2018).

Maintaining plasma membrane integrity is essential to preventing cell death and avoiding the inhibition of root elongation under aluminum stress (Panda & Baluška 2015). In aluminum-tolerant genotypes, the capacity to replace damaged cells enables continued root growth. Conversely, increased cell mortality is associated with the suppression of root elongation in susceptible genotypes (Kariya et al. 2017).

Aluminum tolerance plays a crucial role in plant adaptation to adverse soil conditions and has a direct impact on yield. Therefore, understanding the mechanisms by which aluminum affects membrane integrity and induces cell death is essential for breeding programs. This knowledge enables the identification of tolerance-associated genes and supports the development of improved cultivars.

The Evans blue dye is a well-established, fast and reproducible method for microscopic detection of cell death (Jacyn-Baker & Mock 1994). In turn, machine learning methods offer enhanced diagnostic accuracy, if compared to traditional qualitative analyses by managing complex, non-linear data structures (Gutierrez 2015). These techniques are increasingly applied in agriculture for tasks such as classification, estimation and prediction (Kujawa & Niedbala 2021). In this context, the present study aimed to evaluate the performance of machine learning algorithms in the predictive analysis of aluminum ion accumulation sites, using the Evans blue dye in conjunction with root morphology, during the early development of cowpea genotypes.

MATERIAL AND METHODS

The experiment was conducted at the Universidade Estadual de Feira de Santana, in Feira de Santana (Bahia state, Brazil), from October to November 2019.

A completely randomized design was adopted in a 5 × 14 factorial arrangement, comprising five aluminum doses (0, 50, 100, 150 and 200 μM of $AlCl_3 \cdot 6H_2O$), twelve genotypes (MNC06-895-1; MNC06-895-2; MNC06-901-14; MNC06-907-29; MNC06-907-30; MNC06-907-35; MNC06-908-39; MNC06-909-52; MNC06-909-54; MNC06-909-55; MNC06-909-68; MNC06-909-76) and two commercial cowpea cultivars (BRS ITAIM and CB-27), with ten replications, totaling 700 experimental units.

The cowpea seeds were provided by the Empresa Brasileira de Pesquisa Agropecuária (Embrapa). All accessions belonged to the FR-Fradinho commercial subclass. Seeds were harvested from the 2018 crop and stored using hermetic packaging at room temperature.

Prior to sowing, the seeds were disinfected in a 0.5 % sodium hypochlorite solution for 10 min. They were then placed in rolls of germitest paper (50 seeds $roll^{-1}$) moistened with aluminum solutions at a volume equivalent to 2.5 times the dry mass of the paper. The rolls were sealed in transparent plastic bags and incubated in a biological oxygen demand (B.O.D.) chamber at 25 ± 2 ºC, under an 8-h photoperiod. Seedling evaluation was performed on the fifth day (Brasil 2009).

For the assessment of cell death, root tip samples (1.5 cm) were subjected to the Evans blue staining. The samples were immersed in a 0.25 % (w/v) Evans blue solution for 15 min, then rinsed with distilled water (Kato et al. 2007). Stained roots were analyzed under a BA410E digital optical microscope equipped with a Moticam10 Plus 2.0 camera. Dead cells stained blue, with coloration ranging from light blue (indicating low membrane degradation) to dark blue (indicating extensive membrane damage), following the classification proposed by Braccini et al. (2000), with slight modifications (Figure 1).

In addition to visual assessment, the Evans blue dye absorbed by roots was quantified using 1.5-cm root segments from the apex of 10 seedlings per treatment. The dye retained by dead or damaged cells was extracted with 900 μL of dimethyl sulfoxide (DMSO) and incubated for one hour, followed by absorbance measurement using an FEMTO 800XI spectrophotometer at 600 nm (Vijayaraghavareddy et al. 2017).

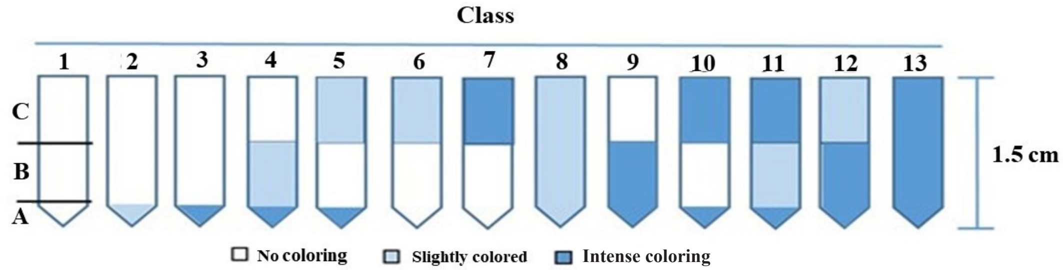

Figure 1. Classes of aluminum accumulation in cowpea roots, adapted using the Evans blue staining of root apices: A) root cap; B) apical meristem (regions of cell division and elongation); C) basal region (maturation zone). Source: adapted from Braccini et al. (2000).

Simultaneously, four machine learning models - Random Forest, Decision Tree, k-Nearest Neighbors (kNN) and Neural Network - were evaluated using the Orange Canvas software. A total of 3,066 images, categorized by five aluminum concentrations, were analyzed. Of these, 3,035 were successfully converted into numerical vectors during the image processing, whereas 31 were excluded due to calculation failure.

The image analysis was performed using the Google's InceptionV3 deep neural network, pre-trained on the ImageNet dataset (Szegedy et al. 2016). This integrated approach enabled a comprehensive analysis of aluminum ion interactions with root morphology in cowpea during early seedling development.

Model performance was evaluated using classification accuracy and the area under the curve, with additional analyses performed through receiver operating characteristic curves and confusion matrices. A stratified 10-fold cross-validation protocol was applied.

For the Random Forest model, 11 decision trees were tested, with five attributes evaluated at each split node. The minimum number of instances per leaf was set at two, and the maximum tree depth was limited to 100. Training was halted when 95 % of the specified maximum depth was reached.

In the kNN model, predictions were based on the average of the closest training examples within the feature space. The Euclidean distance was used as the distance metric, with uniform weighting applied.

For the Neural Network, 48 neurons per hidden layer were employed, with the ReLU activation function. The Adam optimizer (a stochastic gradient-based method) was used for weight optimization, with a regularization parameter (α) of 0.0001 and a maximum of 200 training iterations.

Statistical analyses were conducted with a factorial design in the R software environment (R Core Team 2021) with the ExpDes package (Ferreira et al. 2018). Observed variable values were subjected to analysis of variance (Anova) using the F-test. Significant qualitative effects were compared using the Scott-Knott test, whereas quantitative effects were analyzed through regression, with all tests performed at a significance level of $p < 0.05$.

RESULTS AND DISCUSSION

The presence of blue staining in cowpea root tips following the Evans blue dye application confirmed the occurrence of cell death in response to aluminum exposure (Figure 2).

The CB-27 genotype exhibited intense blue staining at the 200-µM concentration, suggesting a high sensitivity to aluminum ions. In contrast, MNC06-909-52 and MNC06-909-68 showed a lighter blue staining, which may indicate aluminum exclusion mechanisms contributing to greater tolerance. Kariya et al. (2017), in a study on tobacco roots, demonstrated a correlation between increased cell death and reduced root elongation under aluminum exposure.

Understanding mechanisms that alleviate aluminum toxicity - from the root apex to the differentiation zone - is essential. Certain plants release exudates that act as protective agents, mitigating aluminum stress. Sasse et al. (2018) reported that these exudates, despite originating from a small root region, vary in molecular composition. In genotypes with promising tolerance, aluminum ions do not inhibit the number or length of lateral roots, suggesting that aluminum toxicity may primarily target DNA, as supported by Eekhout et al. (2017), who identified *Arabidopsis* mutants with high Al tolerance.

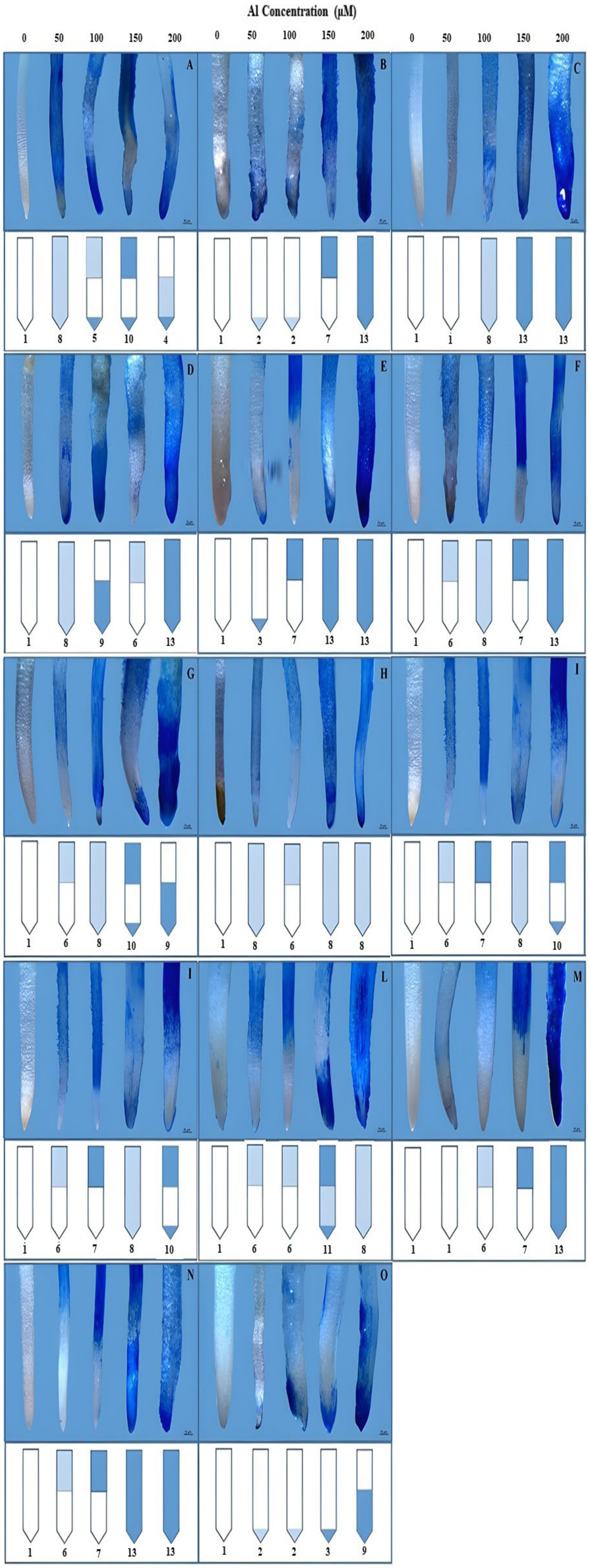

Figure 2. Detection of cell death via the Evans blue staining in root apices of cowpea genotypes after 5 days of aluminum exposure in a B.O.D. chamber. Each row represents a genotype, beginning with the control treatment and followed by increasing Al concentrations.

According to Kochian et al. (2015), plants capable of maintaining growth under aluminum stress often rely on exclusion mechanisms and detoxification or sequestration of internalized Al. The exudation of organic acids such as malate, citrate and oxalate plays a crucial role in mitigating aluminum toxicity and enhancing tolerance (Chauhan et al. 2021, Ofoe et al. 2023).

Yokosho et al. (2016) noted that aluminum tolerance in plants is closely linked to the sequestration of Al ions into vacuoles, thereby reducing cytoplasmic toxicity.

The interaction between genotypes and aluminum concentrations revealed no significant differences among the genotypes in the absence of Al (Table 1). However, at 50, 100, 150 and 200 µM, the genotypes were grouped into 2, 3, 4 and 5 statistically distinct clusters, respectively. At 50 µM, MNC06-908-39 and MNC06-909-55 exhibited a significantly greater dye accumulation. At 100 µM, the genotypes MNC06-909-52, MNC06-909-54, MNC06-909-55, MNC06-909-76 and CB-27 were more sensitive, whereas MNC06-895-2, MNC06-907-29, MNC06-907-35 and BRS ITAIM demonstrated a greater tolerance.

At 150 µM, MNC06-907-29, MNC06-907-35 and BRS ITAIM showed increased tolerance, whereas MNC06-909-55 and CB-27 remained more sensitive. At 200 µM, MNC06-908-39 exhibited the highest Evans blue accumulation, indicating a greater sensitivity, whereas MNC06-907-29 showed the least accumulation, suggesting effective physiological mechanisms such as root exudation for mitigating aluminum toxicity.

Safari et al. (2017) emphasized that aluminum-sensitive plants experience rapid root growth inhibition, even under low Al concentrations, primarily due to damage at the cell wall level. Analyzing the interaction between aluminum concentrations within genotypes (Table 2), all genotypes exhibited significant responses, with a consistent positive linear trend.

The highest relative Evans blue staining, when compared to the control, was observed in the following order: MNC06-908-39 > MNC06-895-1 > MNC06-907-35 = BRS ITAIM > MNC06-909-68 > CB-27 > MNC06-895-2 = MNC06-909-52 > MNC06-907-30 > MNC06-909-55 > MNC06-909-76 > MNC06-909-54 > MNC06-901-14 > MNC06-907-29, with dye accumulation

Table 1. Breakdown of genotype × aluminum concentration interaction for the Evans blue dye accumulation in cowpea root apices.

Genotype	Al concentration (μM)				
	0	50	100	150	200
MNC06-895-1	0.000212 a*	0.000361 b	0.001444 b	0.002442 c	0.004056 c
MNC06-895-2	0.000191 a	0.000934 b	0.000892 c	0.002803 c	0.002761 d
MNC06-901-14	0.000042 a	0.001125 b	0.001975 b	0.002378 c	0.002591 d
MNC06-907-29	0.000382 a	0.000595 b	0.000998 c	0.001019 d	0.001465 e
MNC06-907-30	0.000127 a	0.001041 b	0.001996 b	0.002612 c	0.003122 d
MNC06-907-35	0.000021 a	0.000871 b	0.001125 c	0.001550 d	0.004120 c
MNC06-908-39	0.000191 a	0.002357 a	0.001958 b	0.003037 c	0.010363 a
MNC06-909-52	0.000106 a	0.000637 b	0.003058 a	0.003291 c	0.003568 c
MNC06-909-54	0.000064 a	0.001083 b	0.002421 a	0.002463 c	0.004438 c
MNC06-909-55	0.000106 a	0.002612 a	0.003568 a	0.005458 a	0.006434 b
MNC06-909-68	0.000234 a	0.001210 b	0.001593 b	0.003865 b	0.003992 c
MNC06-909-76	0.000085 a	0.001444 b	0.002655 a	0.002718 c	0.003355 c
BRS ITAIM	0.000340 a	0.000807 b	0.000977 c	0.002039 d	0.003950 c
CB-27	0.000403 a	0.001487 b	0.002548 a	0.005118 a	0.005713 b

* Different letters in the columns indicate significant differences according to the Scott-Knott test ($p \leq 0.05$).

Table 2. Breakdown of aluminum concentration × genotype interaction for the Evans blue dye accumulation in cowpea root apices.

Genotype	Equation	R^2 (%)
MNC06-895-1	$Y^{**} = 0.0003 + 0.00002x$	93.0
MNC06-895-2	$Y^{**} = 0.0001 + 0.00001x$	86.0
MNC06-901-14	$Y^{**} = 0.0004 + 0.00001x$	95.0
MNC06-907-29	$Y^{*} = 0.0004 + 0.000005x$	95.0
MNC06-907-30	$Y^{**} = 0.0003 + 0.00002x$	98.0
MNC06-907-35	$Y^{**} = 0.0002 + 0.00005x$	82.0
MNC06-908-39	$Y^{**} = 0.0006 + 0.00004x$	71.0
MNC06-909-52	$Y^{**} = 0.0002 + 0.00002x$	86.0
MNC06-909-54	$Y^{**} = 0.00007 + 0.00002x$	94.0
MNC06-909-55	$Y^{**} = 0.0005 + 0.00003x$	97.0
MNC06-909-68	$Y^{**} = 0.0001 + 0.00002x$	92.0
MNC06-909-76	$Y^{**} = 0.0005 + 0.00002x$	90.0
BRS ITAIM	$Y^{**} = 0.00007 + 0.00002x$	85.0
CB-27	$Y^{**} = 0.0002 + 0.00003x$	96.0

** and *: significant at 1 and 5 % of probability, respectively.

percentages of 108, 105, 102, 102, 98, 97, 95, 95, 93, 92, 89, 85, 83 and 71 %, respectively. MNC06-908-39 accumulated substantial dye due to extensive cell death (Figure 2G), whereas MNC06-907-29 (Figure 2D) showed a minimal dye increase across aluminum concentrations.

As noted by Panda & Baluška (2015), aluminum tolerance may preserve membrane integrity and reduce cell death, thereby minimizing root elongation inhibition.

Giannakoula et al. (2010) found significantly higher aluminum accumulation in sensitive maize genotypes, when compared to tolerant ones, after 72 hours of exposure. Once inside the plant tissues, aluminum can interact with membrane phospholipids and proteins, altering permeability and impairing water uptake. These effects have been observed in various species, including alfalfa (*Medicago sativa* L.) (Cui et al. 2017), sorghum (*Sorghum bicolor* L. Moench) (Zhou et al. 2017), rye (*Secale cereale*) (Sousa et al. 2016) and chickpea (*Cicer arietinum*) (Sharma et al. 2016).

The Neural Network model demonstrated a precision of 0.724 for true positives among the predicted positive cases, indicating a high classification accuracy (Table 3).

When analyzing aluminum concentrations in cowpea genotypes using the receiver operating characteristic curve (Figure 3), the Neural Network model demonstrated the best overall performance, when compared to the Random Forest, Decision Tree and k-Nearest Neighbors (kNN) models. This is evidenced by the curve's proximity to the upper left corner of the receiver operating characteristic space, indicating a high test accuracy.

The confusion matrix for the Neural Network model (Figure 4) presents the frequency of correctly and incorrectly classified instances across the evaluated aluminum concentrations. This tool is

Table 3. Results of algorithm classification tests.

Predictive model	Accuracy (%)	Precision
Random Forest	57.2	0.570
Decision Tree	53.4	0.534
k-Nearest Neighbors	68.8	0.697
Neural Network	72.4	0.724

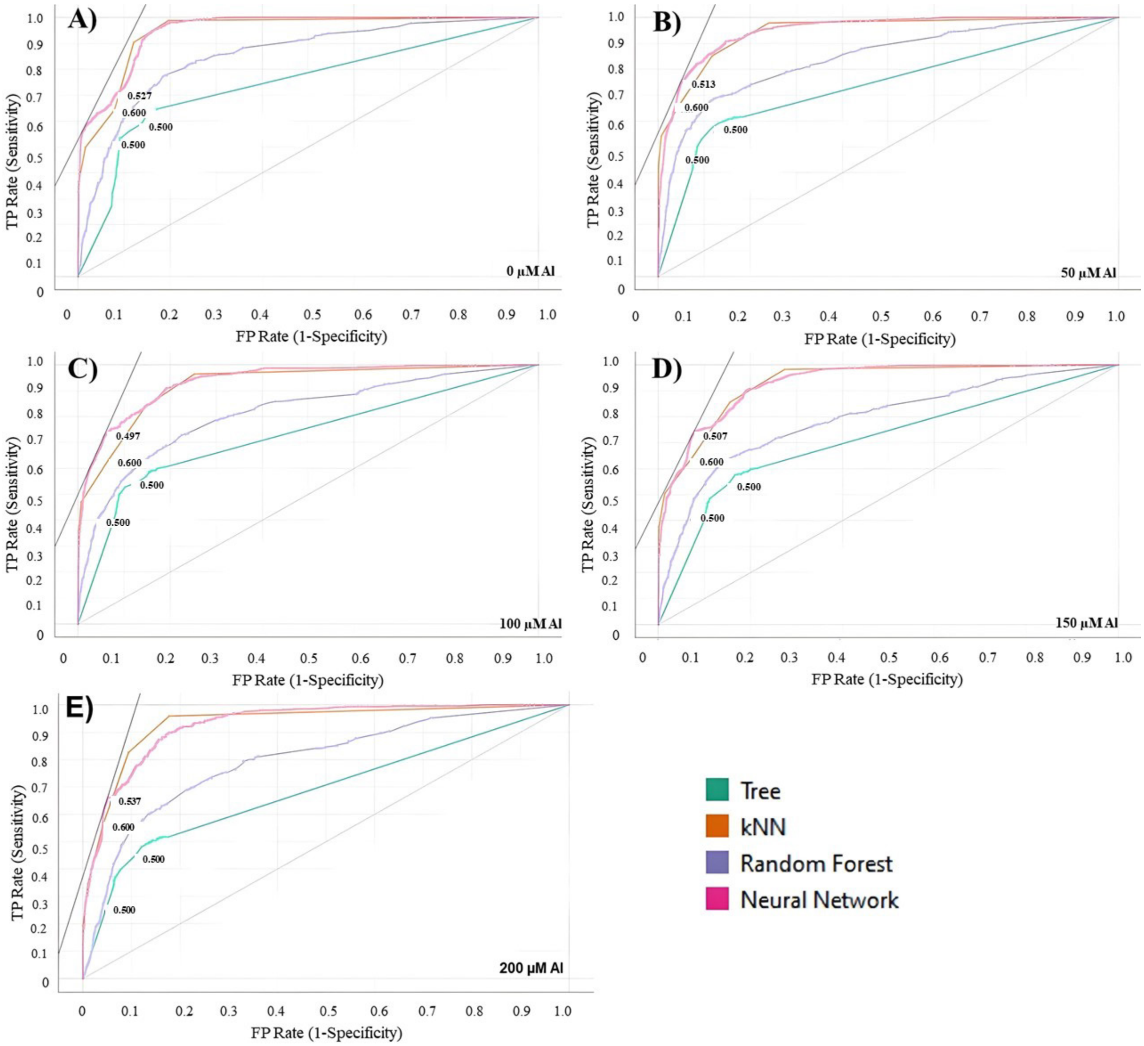

Figure 3. Receiver operating characteristic curve analysis for aluminum ion concentration. TP: true positive; FR: false positive rate.

Concentration (Actual \ Predicted)	0	100	150	200	50	Σ
0	472	65	67	15	47	666
100	73	455	27	40	20	615
150	67	21	506	60	28	682
200	16	47	70	303	30	466
50	52	27	33	33	461	606
Σ	680	615	703	451	586	

Figure 4. Confusion matrix showing the number of correctly and incorrectly classified instances by the Neural Network model.

essential in evaluating model performance, especially in classification problems involving multiple categories. Baryshev et al. (2020) underscore the importance of testing various algorithms on the same dataset, as results may differ significantly depending on model architecture and data characteristics.

The analysis of the confusion matrix indicates that the 150-µM aluminum dose yielded the highest classification reliability, followed by the 0, 50 and 100-µM treatments. In contrast, the 200-µM dose showed the lowest reliability, with an estimated misclassification rate of approximately 25 %, highlighting potential challenges in predictive accuracy at extreme stress levels.

CONCLUSIONS

1. The MNC06-907-29, MNC06-909-52 and CB-27 genotypes demonstrated the greatest tolerance to aluminum toxicity, whereas MNC06-909-54,

MNC06-909-55, MNC06-907-35, MNC06-908-39 and MNC06-909-76 exhibited a greater sensitivity, as revealed through the Evans blue staining;
2. The quantitative analysis of the Evans blue dye accumulation identified the MNC06-907-29 and MNC06-901-14 genotypes as the most aluminum-tolerant ones, confirming their potential for further breeding efforts;
3. The quantification of the Evans blue dye provided a more accurate and objective assessment of cell death than visual evaluation alone, improving genotype classification;
4. Among the tested machine learning algorithms, the Neural Network model exhibited the highest predictive performance, making it the most suitable tool for aluminum stress analysis in cowpea seedlings under the conditions of this study.

ACKNOWLEDGMENTS

The authors acknowledge the Coordenação de Aperfeiçoamento de Pessoal de Nível Superior - Brazil (Capes), for financial support (Funding Code 001).

REFERENCES

BARYSHEV, D. D.; BARYSHEV, N. N.; PRONIN, S. P.; NIKOL'SKII, O. K. Comparison of machine learning methods for solving the problem of wheat seeds classification by yield properties. *Russian Agricultural Sciences*, v. 46, n. 4, p. 410-417, 2020.

BRACCINI, M. C. L.; MARTINEZ, H. E. P.; SILVA, E. A. M.; BRACINNI, A. L.; SCAPIM, C. A. Crescimento da planta e coloração das raízes com hematoxilina como critérios de avaliação de genótipos de café quanto à tolerância à toxidez por alumínio. *Revista Brasileira de Ciência do Solo*, v. 24, n. 1, p. 59-68, 2000.

BRASIL. Ministério da Agricultura, Pecuária e Abastecimento. *Regras para análise de sementes*. Brasília, DF: MAPA/ACS, 2009.

CHAUHAN, D. K.; YADAV, V.; VACULÍK, M.; GASSMANN, W.; PIKE, S.; ARIF, N.; SINGH, V. P.; DESHMUKH, R.; SAHI, S.; TRIPATHI, D. K. Aluminum toxicity and aluminum stress-induced physiological tolerance responses in higher plants. *Critical Reviews in Biotechnology*, v. 41, n. 5, p. 715-730, 2021.

COMPANHIA NACIONAL DE ABASTECIMENTO (Conab). *Acompanhamento da safra brasileira de grãos*: sétimo levantamento: safra 2018/19. 2018. Available at: http://www.conab.gov.br. Access on: Sep. 29, 2020.

CUI, W.; CAO, H.; YAO, P.; PAN, J.; GU, Q.; WANG, R.; OUYANG, Z.; WANG, Q.; SHEN, W. Methane enhances aluminum resistance in alfalfa seedlings by reducing aluminum accumulation and reestablishing redox homeostasis. *Biometals*, v. 30, n. 5, p. 719-732, 2017.

EEKHOUT, T.; LARSEN, P.; VEYLDER, L. de. Modification of DNA checkpoints to confer aluminum tolerance. *Trends in Plant Science*, v. 22, n. 2, p. 102-105, 2017.

FERREIRA, E. B.; CAVALCANTI, P. P.; NOGUEIRA, D. A. *Package 'ExpDes.pt'*: experimental designs: R package version 1.2.0. 2018. Available at: https://cran.r-project.org/web/packages/ExpDes.pt/. Access on: Sep. 29, 2019.

FOOD AND AGRICULTURE ORGANIZATION OF THE UNITED NATIONS (FAO). *Faostat*. 2017. Available at: http://faostat.fao.org/site/567/DesktopDefault.aspx?PageID=567#ancor. Access on: Sep. 29, 2019.

GIANNAKOULA, A.; MOUSTAKAS, M.; SYROS, T.; YUPSANIS, T. Aluminum stress induces up-regulation of an efficient antioxidant system in the Al-tolerant maize line but not in the Al-sensitive line. *Environmental and Experimental Botany*, v. 67, n. 3, p. 487-494, 2010.

GUTIERREZ, D. D. *Machine learning and data science*: an introduction to statistical learning method with R. Basking Ridge: Technics Publications, 2015.

HASSANPOUR, P.; PANAHI, Y.; EBRAHIMI-KALAN, A.; AKBARZADEH, A.; DAVARAN, S.; NASIBOVA, A. N.; KHALILOV, R.; KAVETSKYY, T. Biomedical applications of aluminium oxide nanoparticles. *Micro & Nano Letters*, v. 13, n. 9, p. 1227-1231, 2018.

JACYN-BAKER, C.; MOCK, N. M. An improved method for monitoring cell death in cell suspension and leaf disc assays using Evans blue. *Plant Cell, Tissue and Organ Culture*, v. 39, n. 1, p. 71-12, 1994.

KARIYA, K.; TSUCHIYA, Y.; SASAKI, T.; YAMAMOTO, Y. Aluminum-induced cell death requires upregulation of NtVPE1 gene coding vacuolar processing enzyme in tobacco (*Nicotiana tabacum* L.). *Journal of Inorganic Biochemistry*, v. 181, n. 1, p. 152-161, 2017.

KATO, Y.; MIURA, E.; MATSUSHIMA, R.; SAKAMOTO, W. White leaf sectors in yellow variegated are formed by viable cells with undifferentiated plastids. *Plant Physiology*, v. 144, n. 2, p. 952-960, 2007.

KOCHIAN, L. V.; PIÑEROS, M. A.; LIU, J.; MAGALHÃES, J. Plant adaptation to acid soils: the molecular basis for crop aluminum resistance. *Annual Review of Plant Biology*, v. 66, n. 1, p. 571-598, 2015.

KUJAWA, S.; NIEDBAŁA, G. Artificial neural networks in agriculture. *Agriculture*, v. 11, n. 6, e497, 2021.

OFOE, R.; THOMAS, R. H.; ASIEDU, S. K.; WANG-PRUSKI, G.; FOFANA, B.; ABBEY, L. Aluminum in plant: benefits, toxicity and tolerance mechanisms. *Frontiers in Plant Science*, v. 13, e1085998, 2023.

PANDA, S. K.; BALUŠKA, F. *Aluminum stress adaptation in plants*. Cham: Springer International Publishing, 2015.

R CORE TEAM. *R*: a language and environment for statistical computing. Vienna: R Foundation for Statistical Computing, 2021.

SAFARI, M.; GHANATI, F.; SAFARNEJAD, M. R.; CHASHMI, N. A. The contribution of cell wall composition in the expansion of *Camellia sinensis* seedlings roots in response to aluminum. *Planta*, v. 247, n. 2, p. 381-392. 2017.

SASSE, J.; MARTINOIA, E.; NORTHEN, T. Feed your friends: do plant exudates shape the root microbiome? *Trends in Plant Science*, v. 23, n. 1, p. 25-41, 2018.

SHARMA, M.; SHARMA, V.; TRIPATHI, B. N. Rapid activation of catalase followed by citrate efflux effectively improves aluminum tolerance in the roots of chick pea (*Cicer arietinum*). *Protoplasma*, v. 253, n. 3, p. 709-718, 2016.

SOUSA, A.; ABDELGAWAD, H.; HAN, A.; TEIXEIRA, J.; MATOS, M.; FIDALGO, F. Oxidative metabolism of rye (*Secale cereale* L.) after short term exposure to aluminum: uncovering the glutathione-ascorbate redox network. *Plant Science*, v. 7, e685, 2016.

SZEGEDY, C.; VANHOUCKE, V.; LOFFE, S.; SHLENS, J.; WOJNA, Z. Rethinking the inception architecture for computer vision. *In*: IEEE CONFERENCE ON COMPUTER VISION AND PATTERN RECOGNITION, 2016, Las Vegas. *Proceedings*... Las Vegas: IEEE Computer Society, 2016. p. 2818-2826.

VIJAYARAGHAVAREDDY, P.; ADHINARAYANREDDY, V.; VEMANNA, R. S.; SREEMAN, S.; MAKARLA, U. Quantification of membrane damage/cell death using Evan's blue staining technique. *Bio-Protocol*, v. 7, n. 16, e2519, 2017.

YOKOSHO, K.; YAMAJU, N.; MITANI-UENO, N.; SHEN, R. F.; FENG, J. M. An aluminum-inducible IREG gene is required for internal detoxification of aluminum in buckwheat. *Plant Cell Physiology*, v. 57, n. 6, p. 1169-1178, 2016.

ZHOU, D.; YANG, Y.; ZHANG, J.; JIANG, F.; CRAFT, E.; THANNHAUSER, T. W.; KOCHIAN, L. V.; LIU, J. Quantitative iTRAQ proteomics revealed possible roles for antioxidant proteins in sorghum aluminum tolerance. *Plant Science*, v. 9, n. 7, e2043, 2017.